Electronic Supplementary Information

Controllable dispersion of nickel phthalocyanine molecules on graphene oxide for efficient electrocatalytic CO_2 reduction

Jiaxin He [abd], Yu Han [abd], Xiao Xu [bd], Miao Sun [bd]，Longtian Kang [abd], Wenlie Lin [b*] and Jingjing Liu [c*]*

[a] College of Chemistry, Fuzhou University, Fuzhou 350116, PR China. E-mail: longtiank@fjirsm.ac.cn

[b] State Key Laboratory of Structural Chemistry, and Fujian Provincial Key Laboratory of Nanomaterials, Fujian Institute of Research on the Structure of Matter, Chinese Academy of Sciences, Fuzhou, Fujian 350002, PR China. E-mail: longtiank@fjirsm.ac.cn, Linwenlie@fjirsm.ac.cn

[c] Fujian Universities and Colleges Engineering Research Center of Soft Plastic Packaging Technology for Food, Fujian Polytechnic Normal University, Fuqing, Fujian Province, 350300, P. R. China. E-mail: 116425543@qq.com

[d] University Chinese Academy of Science, Fujian College, Fuzhou 350002, PR China. E-mail: longtiank@fjirsm.ac.cn

Experiment Section

Chemicals and materials

Nickel phthalocyanine (NiPc) with a purity of 92% was purchased from Beijing Bailing Wei Technology Co., Ltd. Flake graphite (2000 mesh) was obtained from Shanghai Aladdin Biochemical Technology Co., Ltd. Reagents, including concentrated sulfuric acid (98%, H_2SO_4), potassium permanganate (99.5%, $KMnO_4$), hydrogen peroxide (99.5%, H_2O_2), and potassium bicarbonate ($KHCO_3$), were sourced from China National Pharmaceutical Group Chemical Reagents Co., Ltd. Ultrapure water was prepared using a purifier (WP-UP-IV20) with a resistivity of 18.25 $M\Omega \cdot cm^{-1}$. All chemicals were used without further purification.

Preparation of Graphene Oxide (GO)

Referring to the preparation methods of GO in the previous studies[1]. GO was obtained by oxidizing natural graphite using an improved Hummer method[2]. Initially, 2.5 g of natural graphite powder and 2.5 g of sodium nitrate ($NaNO_3$) were mixed in a 600 mL beaker. To this mixture, 187.5 mL of concentrated sulfuric acid (H_2SO_4) was added, and the mixture was stirred at room temperature for 24 hours. Subsequently, 11.25 g of potassium permanganate ($KMnO_4$) was slowly introduced into the mixture when maintaining the operation in an ice water bath. The suspension was then stirred at room temperature for 72 hours. Afterward, 250 mL of ultrapure water was added, and the mixture was allowed to cool to room temperature. Then, 22.5 mL of hydrogen peroxide (H_2O_2) was added to the mixture. The brown suspension was centrifuged at 1000 rpm, washed with ultrapure water until the pH is ~7. The final product was dispersed in water to form a GO dispersion system of 1.36 $mg \cdot mL^{-1}$ for further use.

Preparation of NiPc-GO Composites with Different Ratios

Initially, 30.06 mg of NiPc (95%) powder was dissolved in 50 mL of concentrated

sulfuric acid (98%) to yield a 1.0 mM NiPc solution. Next, a 1.36 mg·mL^{-1} GO solution was diluted with deionized water to form 0.1, 0.2, 0.4, 0.6, 0.8 and 1.0 mg·mL^{-1} GO aqueous system. Then, 5 mL GO was transferred into a 15 mL test tube and treated at -2°C for 10 minutes. Following this, 1 mL of the 1 mM NiPc sulfuric acid solution was rapidly injected into the 5 mL GO system with stirring for 25 minutes, and then aged for 3 hours. Finally, the precipitate was separated, washed with ultrapure water, and freeze-dried. The samples were labeled as NiPc-XGO, where X denotes the solid content of GO in water (mg·mL^{-1}). By adjusting the GO solid content, the NiPc-0.1GO, NiPc-0.2GO, NiPc-0.3GO, NiPc-0.4GO, NiPc-0.8GO and NiPc-1.0GO composites were synthesized.

Characterization

Scanning Electron Microscopy (SEM) images were taken using a JSM6700-F (JEOL, Japan).Spherical Aberration Corrected Transmission Electron Microscopy (HADDF-STEM) images were obtained using a JEM-ARM-300F.Structural characterization of the samples was performed using an X-ray diffractometer (XRD; Rigaku, Japan) with Cu Kα radiation (λ=1.54 Å).X-ray Photoelectron Spectroscopy (XPS) characterization was carried out using an ESCALAB 250Xi instrument (Thermon Fisher Scientific, USA) with Al Kα radiation excitation source. Fourier Transform Infrared Spectroscopy (FT-IR) spectra were recorded using a VERTEX70 spectrometer. Raman Spectroscopy was performed using a LABRAM HR Raman spectrometer (HORIBA FRANCE SAS, France) with an excitation wavelength set to 532 nm.

Diffuse Reflectance Infrared Fourier Transform Spectroscopy (DRIFTS) was conducted using a NICOLET-6700 (Thermo Fisher Scientific, USA) spectrometer, equipped with a Mercury Cadmium Telluride-A (MCT-A) probe and a reflection unit for the electrochemical cell at an incident angle of 60°. All tests were performed with a spectral resolution of 4.0 cm^{-1}.Measurements were carried out in an H-type electrochemical cell, using a platinum mesh as the counter electrode and Ag/AgCl as

the reference electrode. The as-synthesized NiPc and NiPc-0.4GO samples were attached to 0.1 × 0.1 cm^2glassy carbon electrodes as working electrodes and tightly attached to the Ge crystal. Prior to test, the probe was cooled with liquid nitrogen for >30 minutes to stabilize the signal. Electrochemical tests were carried out with a CHI760E electrochemical workstation. CO_2 reduction reaction (CO_2RR) measurements were conducted using the timed current method with voltage application. For each measurement, all spectra were subtracted from the background and baseline and calibration was performed on all spectra.

Electrochemical testing

The electrochemical measurements for CO_2RR were performed using a three-electrode system with a CHI760E electrochemical workstation. The custom-made sealed electrolysis H-cell consisted of two chambers separated by a Nafion 117 membrane. Both chambers were filled with 0.1 M $KHCO_3$ solution as the electrolyte, and CO_2 gas was introduced into the cathode chamber at a flow rate of 20 $mL \cdot min^{-1}$ for approximately 30 minutes until saturation at 25°C. A 5.0 mg sample of NiPc-0.4GO catalyst was ultrasonically dispersed in a 1 mL mixture of 975 μL isopropanol and 25 μL Nafion. A uniform 80 μL portion of this dispersion was applied to both sides of a carbon paper, resulting in a loading of 0.2 $mg \cdot cm^{-2}$. The carbon paper was then inserted into a glassy carbon electrode holder to serve as the working electrode. A platinum mesh was used as the counter electrode, and a saturated Ag/AgCl electrode in KCl solution was used as the reference electrode. All potentials were recalibrated to the reversible hydrogen electrode (RHE) scale using the Nernst equation.

$$E\ (vs\ RHE) = E\ (vs\ Ag/AgCl) + 0.197\ V + 0.059\ V \times pH - 0.9 \times IR.^{3}$$

Controlled electrolysis was carried out for 720 seconds at each respective potential before measurements. In the final minute of electrolysis, 1 mL of gas was rapidly extracted from the top space of the electrochemical H-cell using a sealed syringe and injected into a gas chromatograph for analysis. The gas chromatograph was equipped

with a flame ionization detector (FID) and a thermal conductivity detector (TCD). After 1 hour of electrolysis, liquid products were collected and analyzed by NMR with dimethyl sulfoxide (DMSO) as the internal standard. No significant liquid-phase products were detected according to the NMR results. The Faradaic efficiency (FE) was calculated using the following formula:

$$FE_{CO/H2} = \frac{Q_{CO/H_2}}{Q_{total}} = \frac{V_{CO/H_2} \times 2 \times F}{22.4 mol\, L^{-1} \times\ Q_{total}}$$

Where, the Q total was determined by integrating the current over the duration of the electrolysis process.; V represents the volume of gas-phase products flowing into the gas chromatography system. The factor of 2 accounts for the number of electrons transferred in the production of each H_2 or CO molecule, while F denotes the Faraday constant, which is 96,485 C mol^{-1}[1].Each result in this work represents the average of three experimental runs. Electrochemical impedance spectroscopy (EIS) was conducted in 0.1 M $KHCO_3$ with an AC voltage amplitude of 5 mV and a frequency range from 0.1 Hz to 100 kHz to investigate the charge transfer resistance. The stability of the NiPc-0.4GO catalyst was tested during a 26,000-second continuous electrolysis process, with GC measurements taken every 500 seconds to monitor the gas phase composition. The turnover frequency (TOF) for CO formation was calculate as following equation:

$$TOF(s^{-1}) = \frac{J \times S}{N \times F} * \frac{M}{m_{cat*}\omega}$$

J, partial current density for CO production ($A \cdot cm^{-1}$); S, geometric surface area of working electrode (cm^2); N, electron transfer number, which is 2 for CO; F, Faradaic constant, 96485 $C \cdot mol^{-1}$; m_{cat}, mass of catalyst on the electrode (g); ω, loading of single-atom metal in the catalyst; M, atomic mass of single-atom metal ($g \cdot mol^{-1}$).

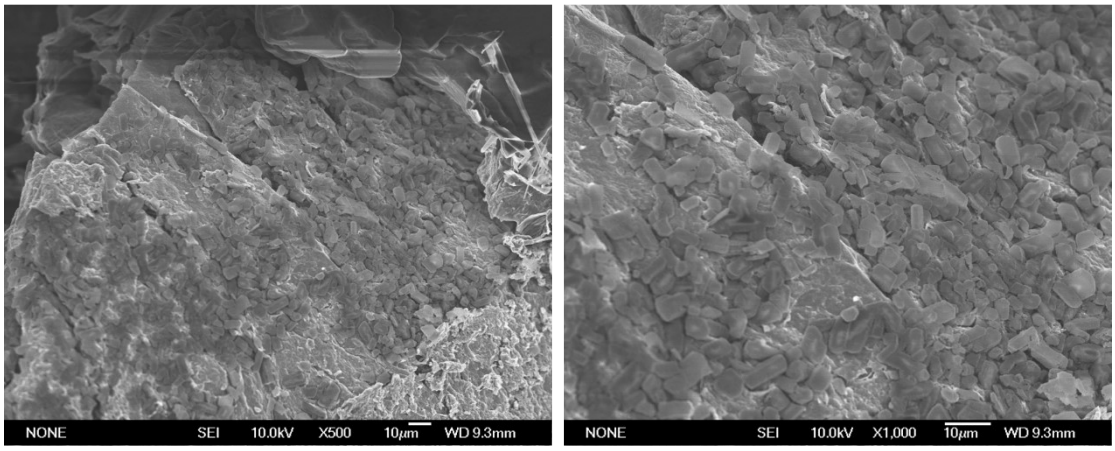

Fig. S1 SEM images of NiPc-0.1GO sample.

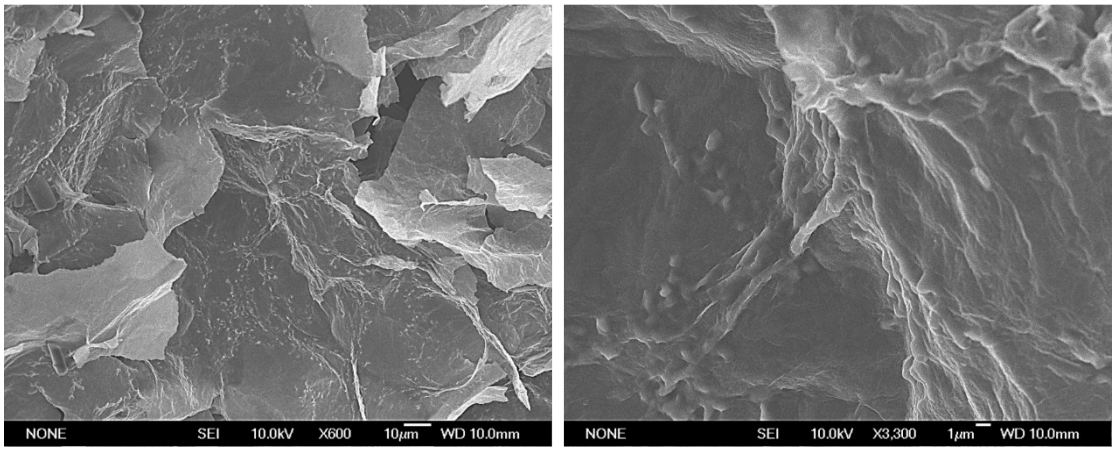

Fig. S2 SEM images of NiPc-0.2GO sample.

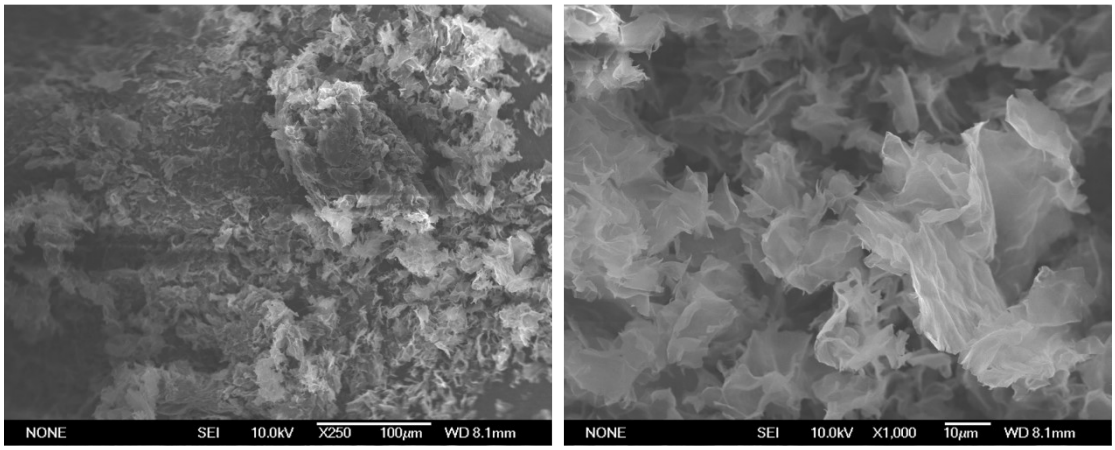

Fig. S3 SEM images of NiPc-0.4GO sample.

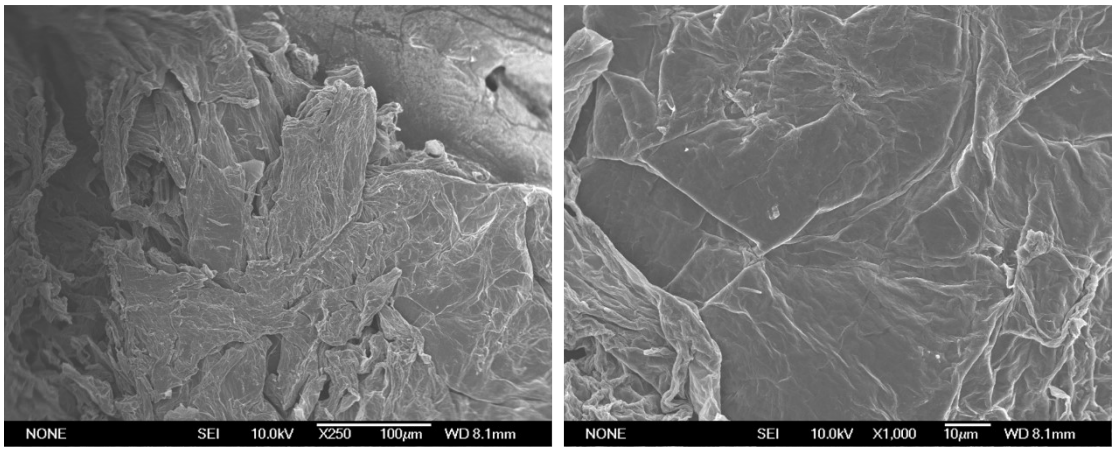

Fig. S4 SEM images of NiPc-0.6GO sample

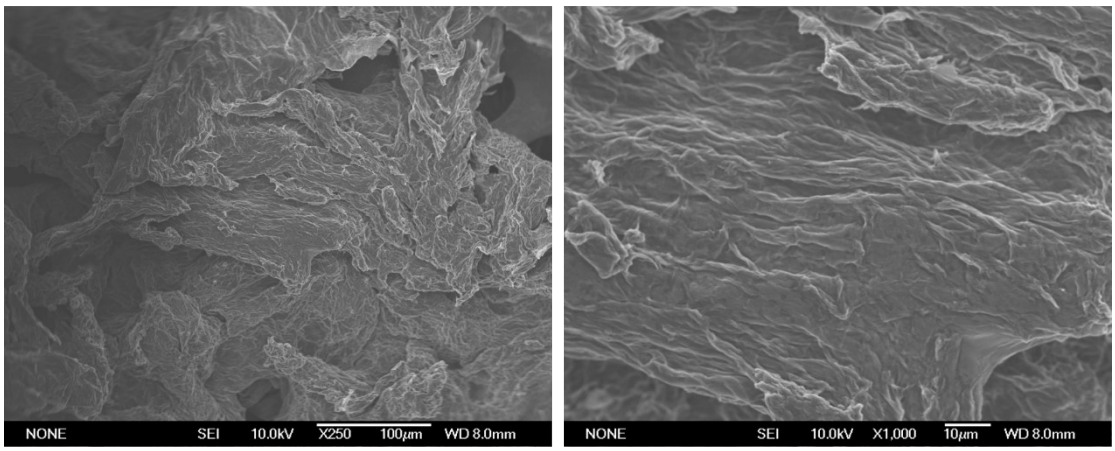

Fig. S5 SEM images of NiPc-0.8GO sample.

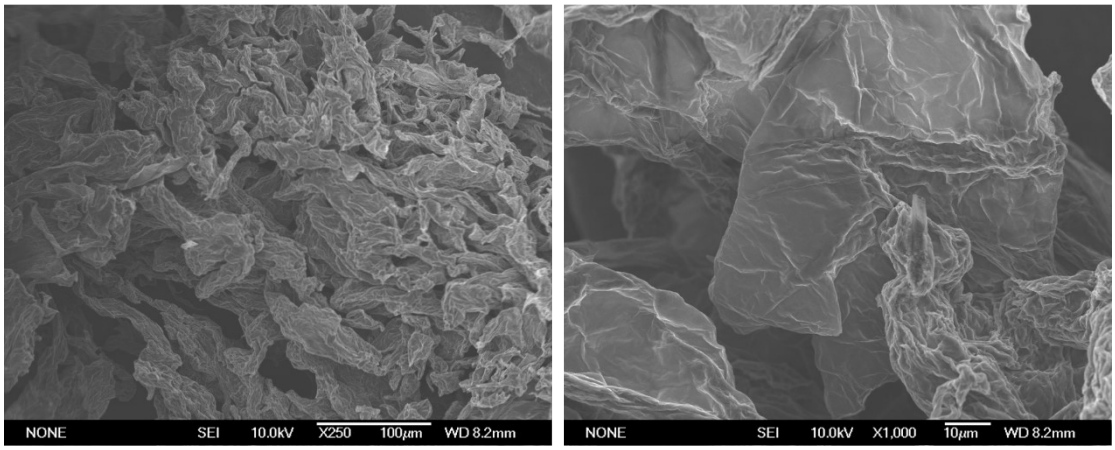

Fig. S6 SEM images of NiPc-1.0GO sample.

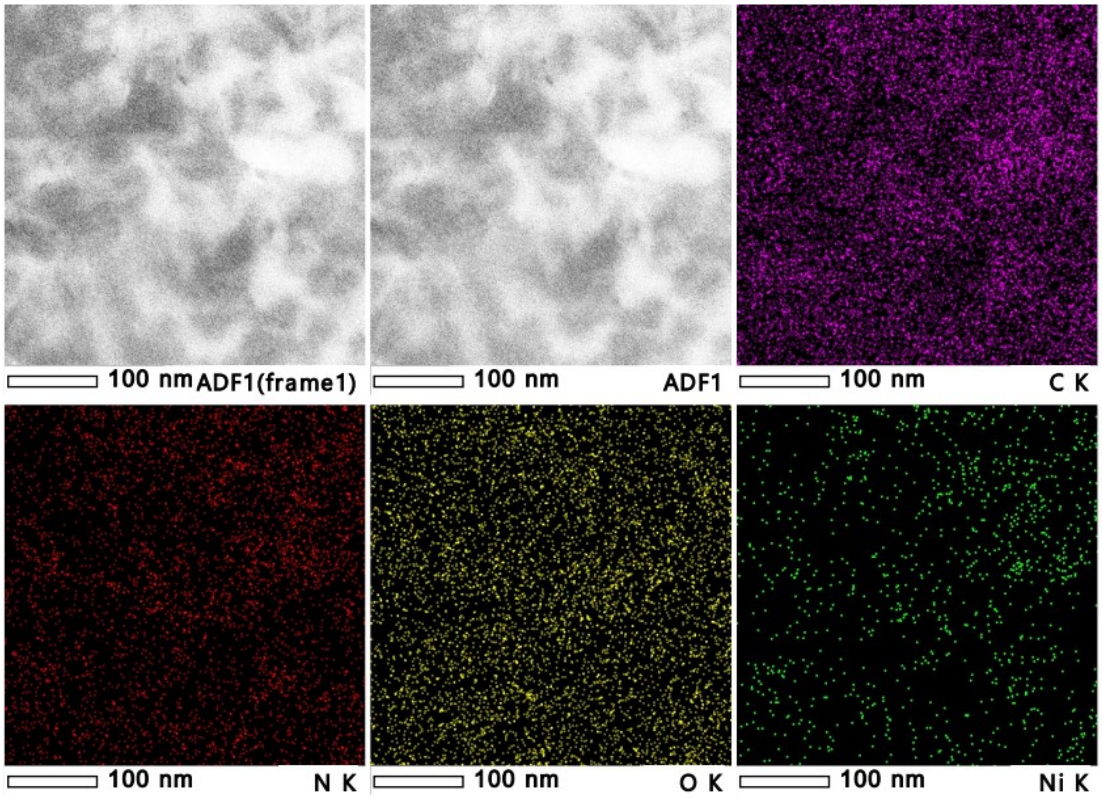

Fig. S7 TEM and Energy dispersive X-ray spectroscopy (EDS) images of NiPc-0.4GO sample.

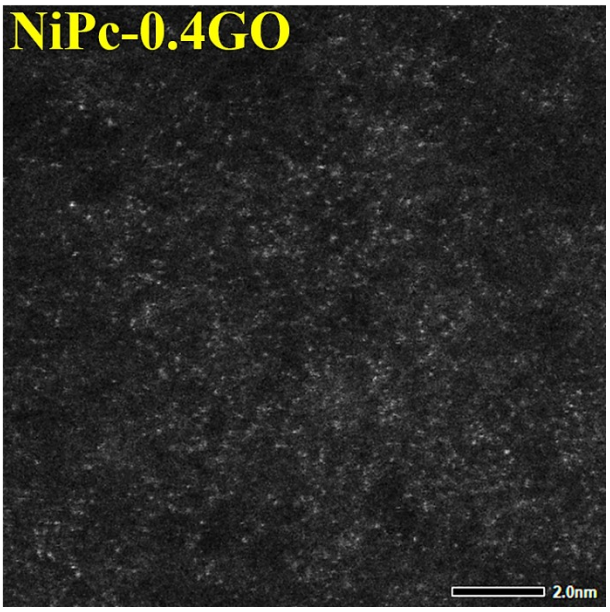

Fig. S8 HAADF-STEM image of NiPc-0.4GO sample.

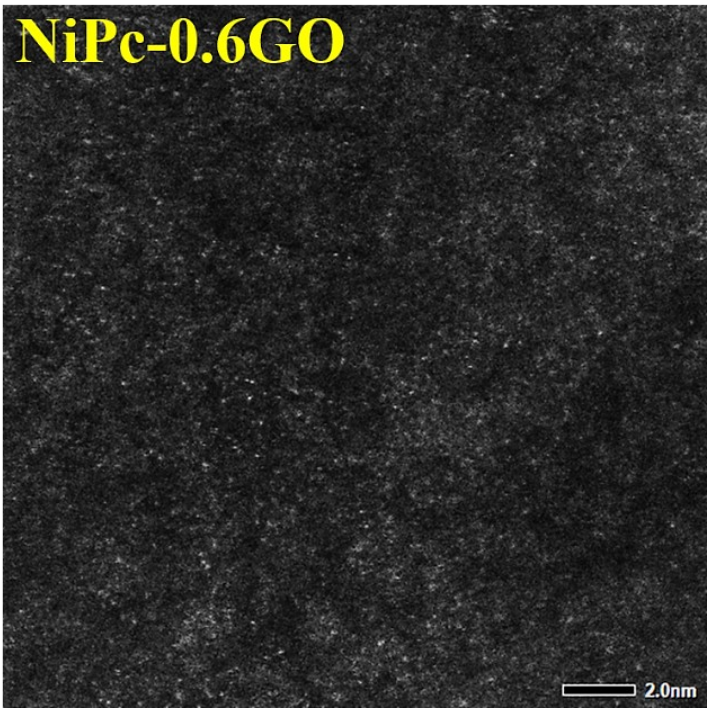

Fig. S9 HAADF-STEM image of NiPc-1.0GO sample.

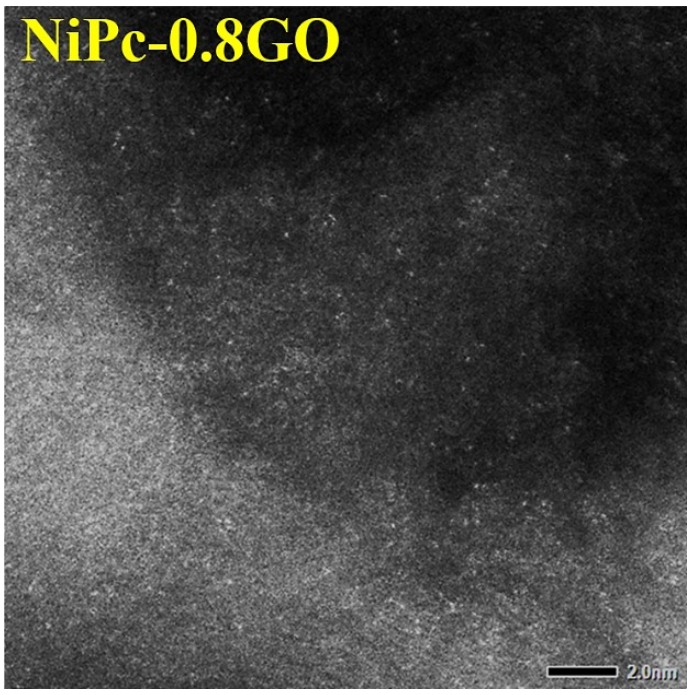

Fig. S10 HAADF-STEM image of NiPc-0.8GO sample.

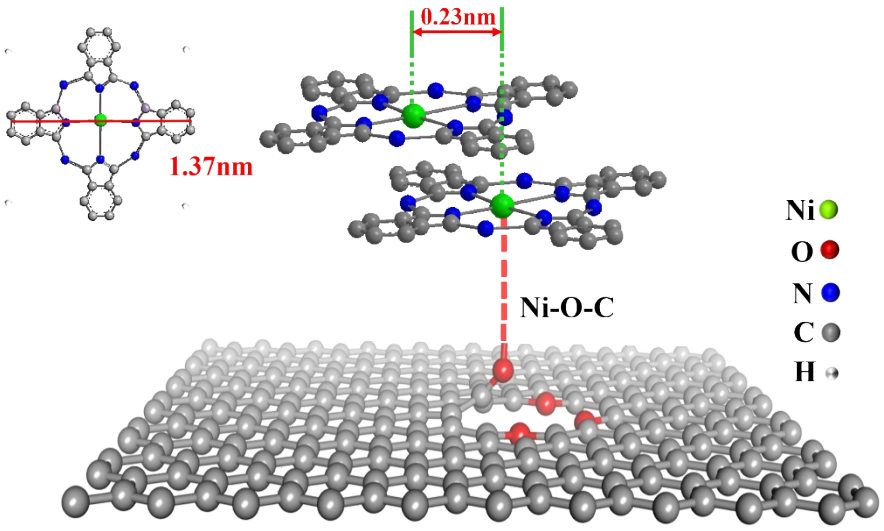

Fig. S11 The structure of Ni(II)/Ni(III)/GO

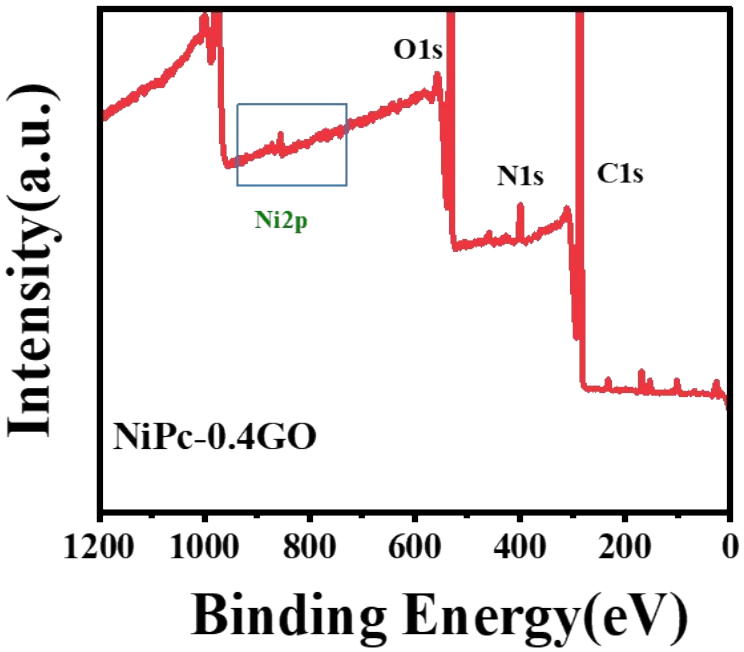

Fig. S12 XPS full spectrum of NiPc-0.4GO

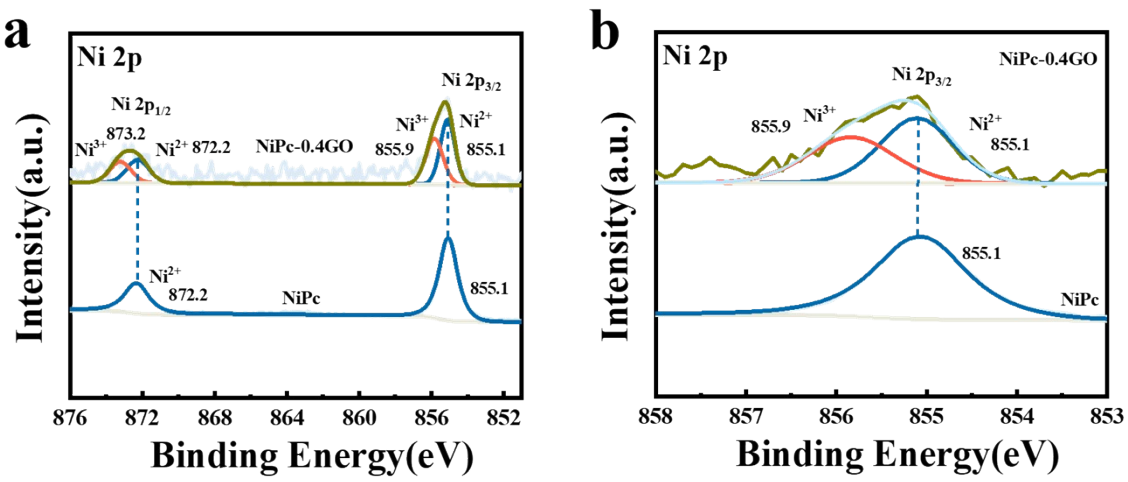

Fig. S13 High resolution XPS spectra of Ni 2p (a) and $Ni2p_{2/3}$ (b) of NiPc and NiPc-0.4GO

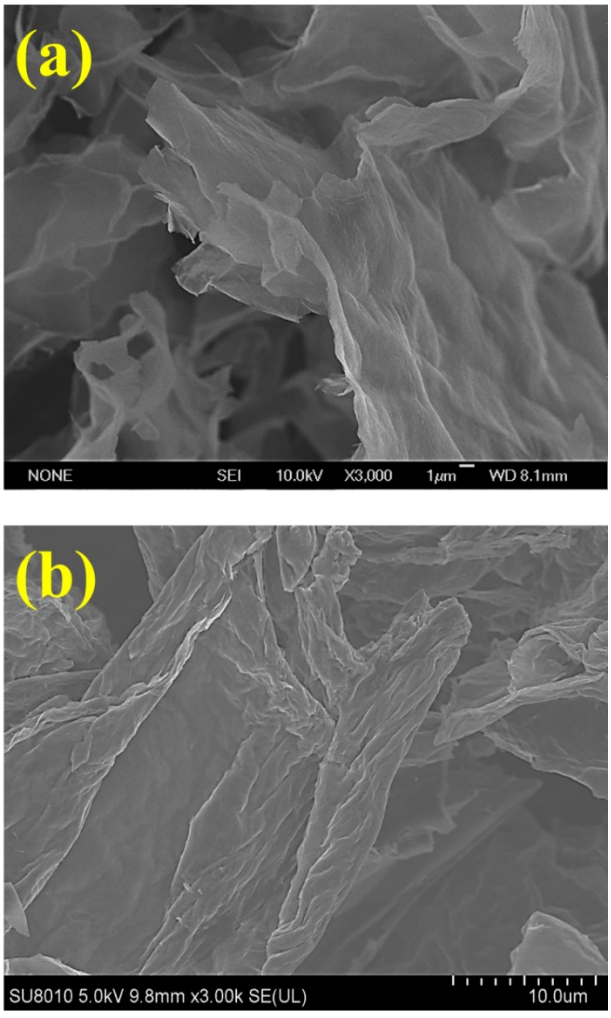

Fig. S14 SEM images of NiPc-0.4GO before (a) /after (b) ECO_2RR test

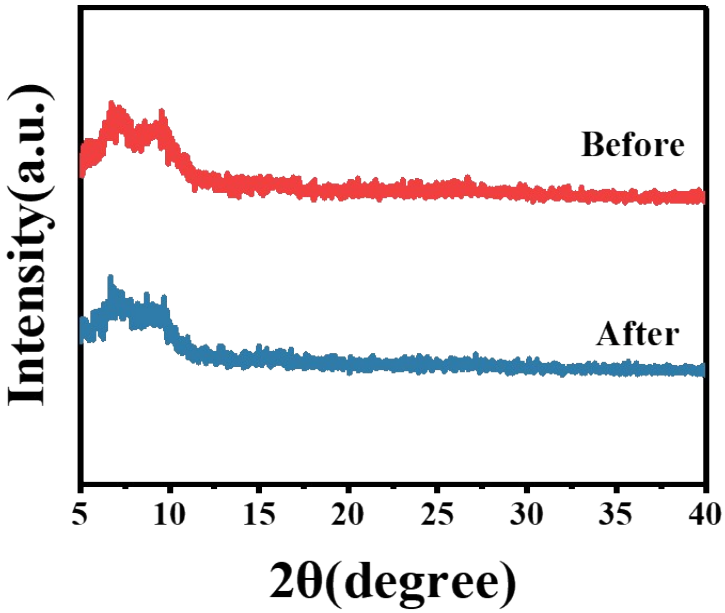

Fig. S15 XRD patterns of NiPc-0.4GO after/before ECR test

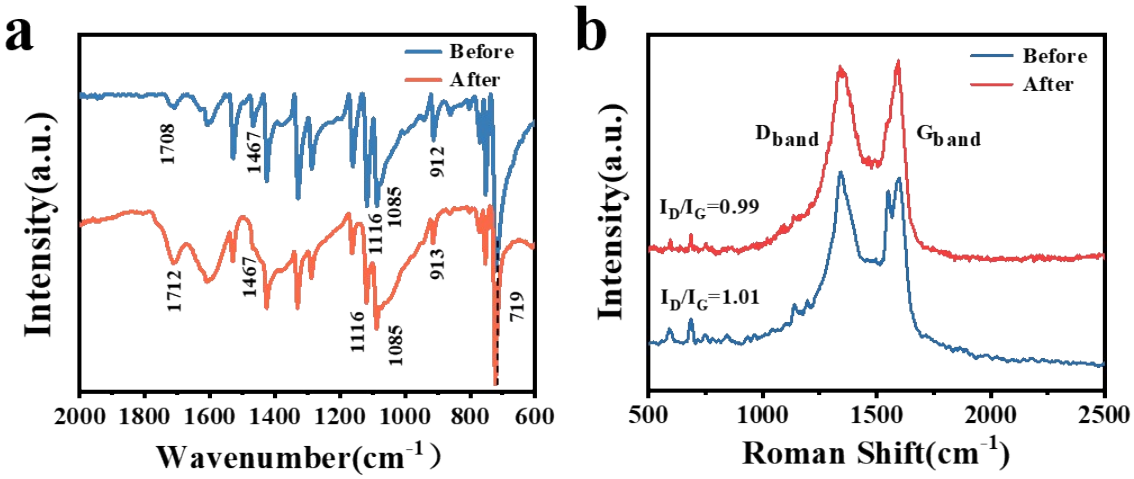

Fig. S16 FT-IR spectra(a) and (b) Raman spectra of NiPc-0.4GO samples before/after ECO_2RR test

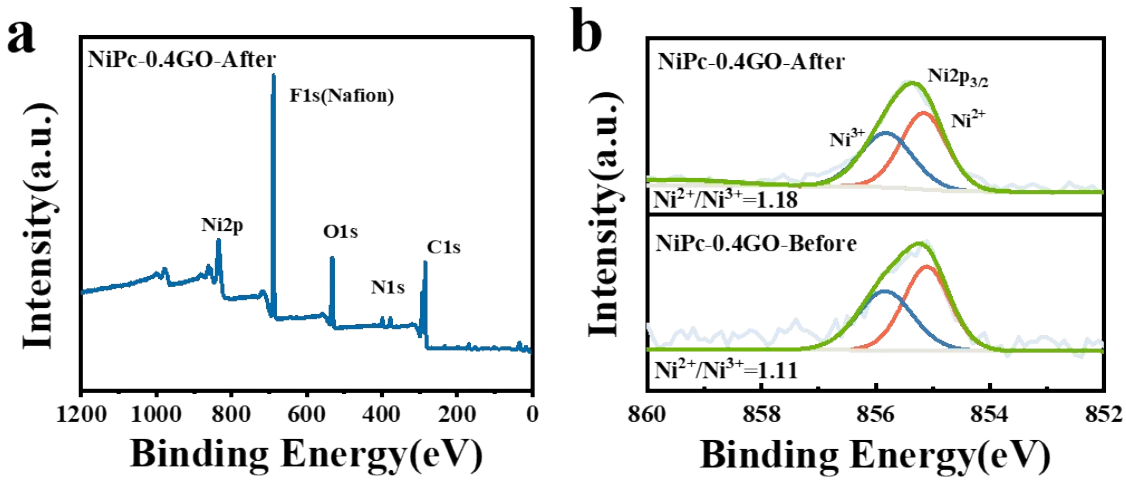

Fig. S17 Full XPS spectra(a) and High-resolution XPS spectra of Ni 2p (b) of NiPc-0.4GO samples before/after ECO_2RR test.

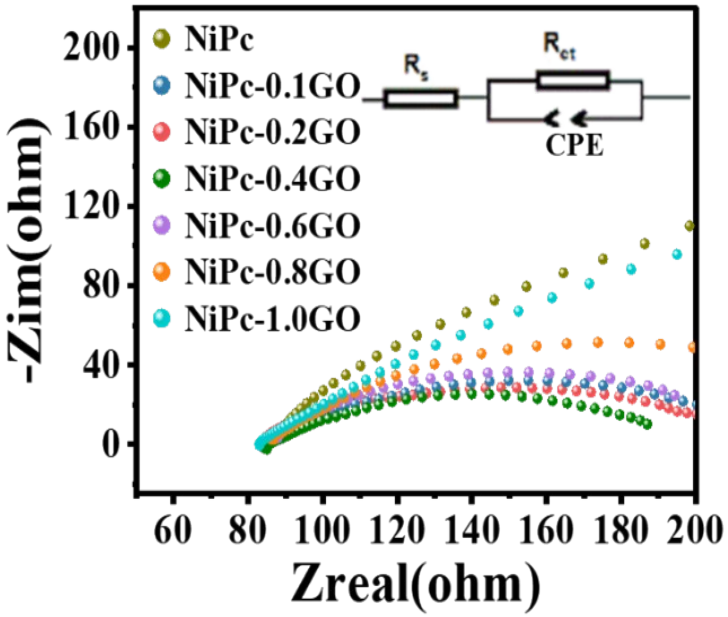

Fig. S18 EIS plots of NiPc, NiPc-0.1GO, NiPc-0.2GO, NiPc-0.4GO, NiPc-0.6GO, NiPc-0.8GO, and NiPc-1.0GO

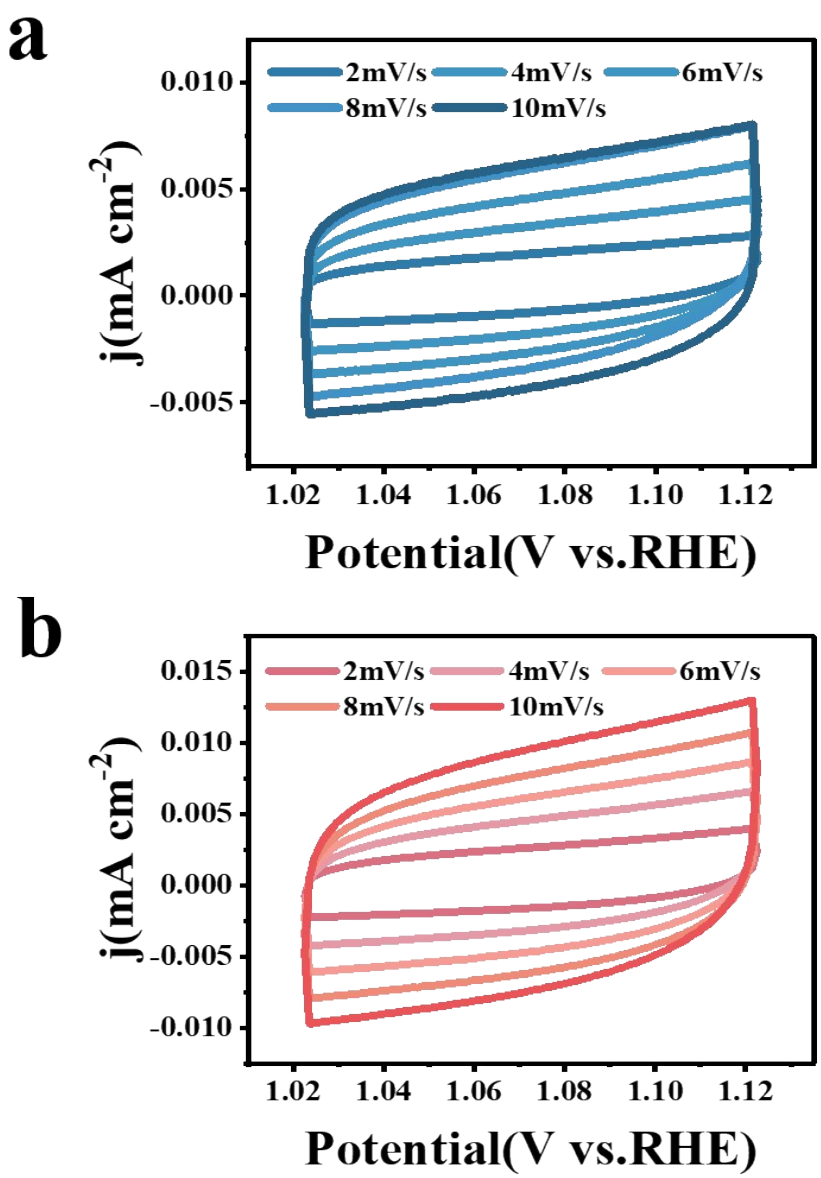

Fig. S19 Cyclic voltammograms of NiPc (a) and NiPc-0.4GO (b) catalysts at scan rates of 2, 4, 6, 8, and 100 mV·s^{-1}, recorded in the potential range from 1.02 to −1.22 V.

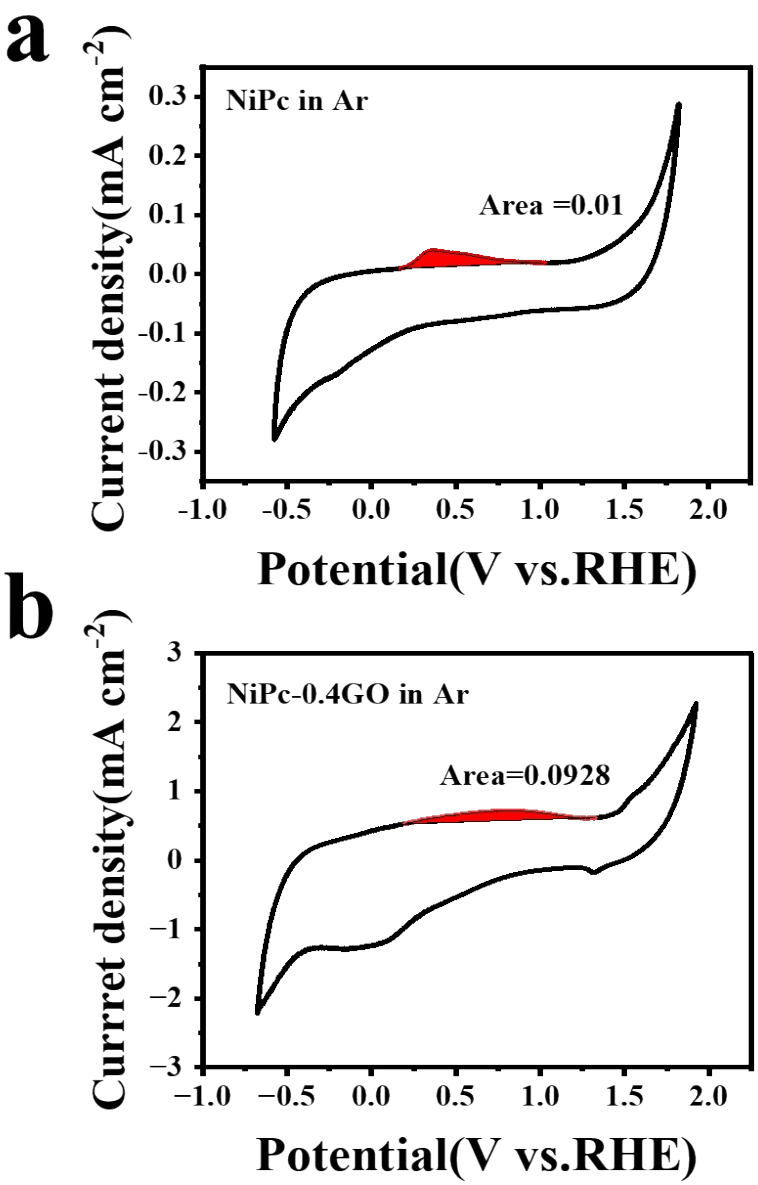

Fig. S20 Cyclic voltammograms of (a) NiPc and (b) NiPc-0.4GO in saturated 0.1 M $KHCO_3$ under an Ar atmosphere. The red region represents the total charge of the anodic wave.

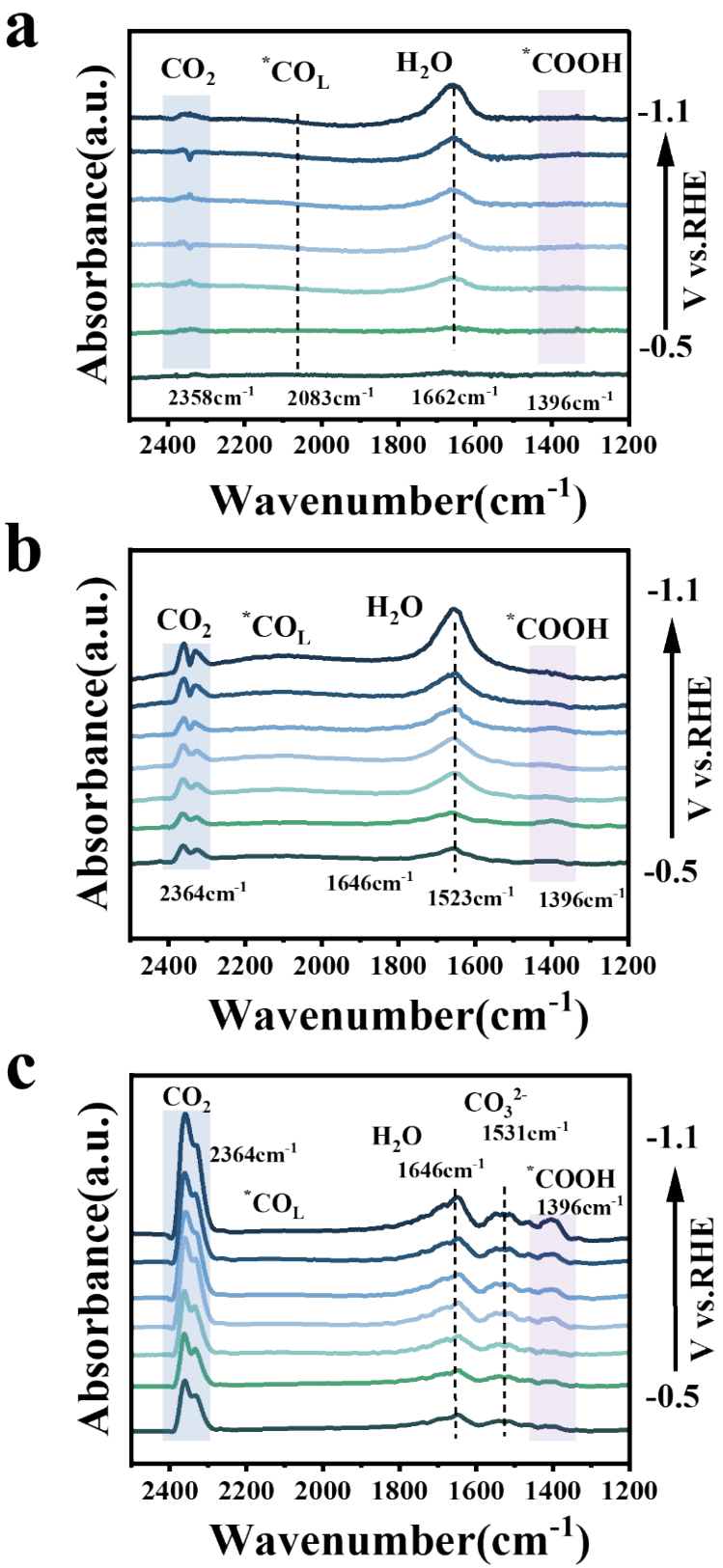

Fig. S21 In-situ DRIFTS spectra for CO_2RR of (a) NiPc, (b) NiPc-0.1GO and (c) NiPc-1.0GO samples at different work potentials.

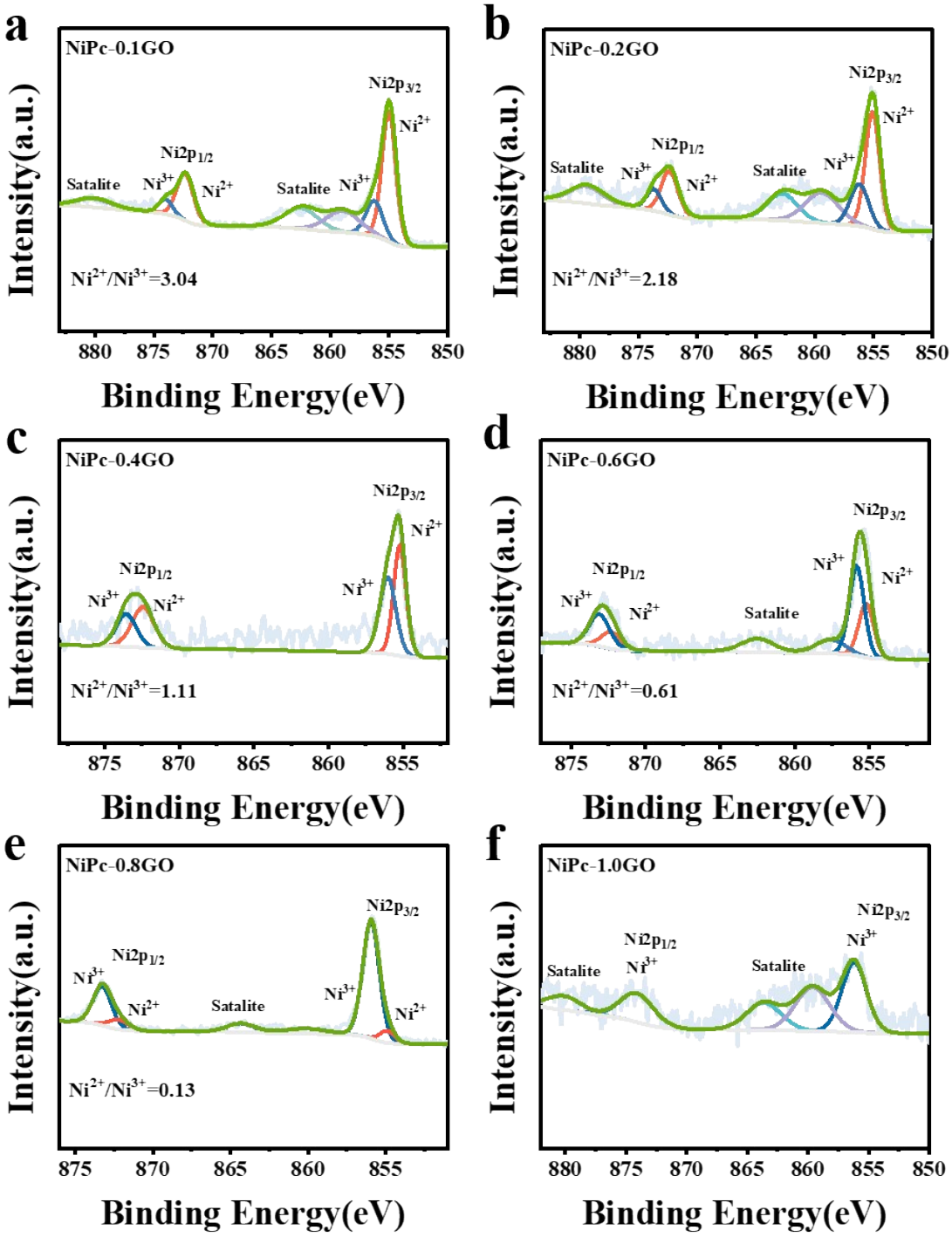

Fig. S22 High-Resolution XPS Spectra of (a) NiPc-0.1GO, (b) NiPc-0.2GO, (c) NiPc-0.4GO, (d) NiPc-0.6GO, (e) NiPc-0.8GO, (f) NiPc-1.0GO.

Table S1 Faraday efficiency of the samples at different potentials (V_{RHE}).

Samples	-0.6 V		-0.7 V		-0.8 V		-0.9 V		-1.0 V		-1.1 V	
	CO	H_2	CO	H_2	CO	H_2	CO	H_2	CO	H_2	CO	H_2
NiPc	12.8	82.7	34.3	65.7	41.2	58.8	45.5	54.5	23.2	76.8	12.5	87.5
NiPc-0.1GO	22.6	77.4	50.2	49.8	69.1	30.9	70.7	29.3	36.6	63.4	23.3	76.6
NiPc-0.2GO	47.8	52.2	70.2	29.8	82.4	17.6	85.9	14.1	78.2	21.8	55.4	44.6
NiPc-0.4GO	76.4	23.6	90.5	9.5	95.7	4.3	98.6	1.4	97.1	2.9	96.8	3.2
NiPc-0.6GO	73.2	26.8	89.4	10.6	93.5	6.5	94.8	5.2	95.7	4.3	92.4	7.6
NiPc-0.8GO	58.6	41.4	80.2	19.8	88.7	11.3	91.3	8.7	90.8	9.2	89.7	10.3
NiPc-1.0GO	51.7	48.3	58.2	41.8	64.8	35.2	69.1	30.9	67.4	32.6	64.3	35.7

Table S2 Summary of recently reported electrocatalysts for CO_2RR

Electrocatalysts	Mass loading [mg cm^{-2}]	Electrolyte	J_{CO} [mA cm^{-2}]	Faradaic Efficiency (>90%, potential range)	Stability [h]	Ref.
NiPc−0.4GO	0.2	0.1 M $KHCO_3$	6.4	(−0.9 V, ~99%) (−0.6 V to −1.1V), >90%	6	**This work**
NiPc/NC	1	0.5 M $KHCO_3$	7.5	(−0.7 V, ~98%) (−0.5 V to −0.8V), >93%	7	[4]
NiPc/N−mG (900)	0.5	0.1 M $KHCO_3$	7.8	(−0.9 V, ~96%) (−0.5 V to −1.1 V), >90%	10	[5]
Ni−N−CNTs−10	5	0.5 M $KHCO_3$	5.3	(−0.65 V, ~98%) (−0.57 V to −0.81V),>80%	20	[6]
Fe_1−Ni_1−N−C	5	0.5 M $KHCO_3$	2.4	(−0. 5 V, ~96%） (−0.4 V to −0.6V), >90%	10	[7]
NiPPc−CB−p800	0.38	0.5 M $KHCO_3$	7.8	(−0.6 V, ~95%) (−0.55 V to −0.7 V), >90%	7	[8]
NiPc−NC	4	0.5 M$KHCO_3$	12	(−0.8 V, ~96%) (−0.7 V to −0.95V), >92%	12	[9]
NiPc/NH_2−CNT	0.5	0.5 M $KHCO_3$	3.16	(−0.6 V, ~96%) (−0.5 V to −0.8V), >90%	7	[10]
NiPc(α−NO_2)$_4$/CNT	/	0.1 M $KHCO_3$	7	(−1.0 V, ~98%) (−0.7 V to −1.2V), >92%	5.5	[11]
0.5NiPc−COF	/	0.5 M $KHCO_3$	13.6	(−0.8 V, ~95%) (−0.8 V to −0.9V), >90%	14	[12]
Ni−NC/NHCSs−−600	/	0.5 M $NaHCO_3$	14.2	(−0.87 V, ~95%) (−0.57 V to −1.07V),>90%	14	[13]

Table S3 The positions of Ni^{2+} and Ni^{i3+} orbital peaks in the Ni 2p XPS spectra of a series of complexes and their component contents.

Sample	Ni^{2+} $2p_{3/2}$		Ni^{3+} $2p_{3/2}$		Ratio of Ni^{2+}/Ni^{3+}
	Binding Energy (eV)	Content (%)	Binding Energy (eV)	Content (%)	
NiPc	855.1	82.08	855.9	/	100% Ni^{2+}
NiPc−0.1GO	855.1	35.26	855.9	11.59	3.04
NiPc−0.2GO	855.1	13.91	855.9	6.38	2.18
NiPc−0.4GO	855.1	33.27	855.9	29.97	1.11
NiPc−0.4GO-After ECO_2RR	855.1	30.05	855.9	25.47	1.18
NiPc−0.6GO	855.1	20.34	855.9	33.35	0.61
NiPc−0.8GO	855.1	6.77	855.9	52.12	0.13
NiPc−1.0GO	855.1	27.12	855.9	100	100% Ni^{3+}

References

1. X. Li, G. Chai, X. Xu, J. Liu, Z. Zhong, A. Cao, Z. Tao, W. You and L. Kang, *Carbon*, 2020, **167**, 658-667.
2. X. Yan, X. Xu, Q. Liu, J. Guo, L. Kang and J. Yao, *J. Power Sources*, 2018, **389**, 260-266.
3. S. Min, X. Xu, J. He, M. Sun, W. Lin and L. Kang, *Small*, 2024, **20**, 2400592.
4. X. Yang, J. Cheng, X. Xuan, N. Liu and J. Liu, *ACS Sustain. Chem. Eng.*, 2020, **8**, 10536-10543.
5. Y. Choi, K.-W. Kim, B. J. Park, T. Y. Kim, Y. Lee, B. Park, J. K. Kim and J. W. Han, *J. Mater. Chem. A*, 2025, **13**, 4861-4869.
6. S. Wu, F. Yi, D. Ping, S. Huang, Y. Zhang, L. Han, S. Wang, H. Wang, X. Yang, D. Guo, G. Liu and S. Fang, *Carbon*, 2022, **196**, 1-9.

7. L. Jiao, J. Zhu, Y. Zhang, W. Yang, S. Zhou, A. Li, C. Xie, X. Zheng, W. Zhou, S.-H. Yu and H.-L. Jiang, *J. Am. Chem. Soc*, 2021, **143**, 19417-19424.
8. J. Chen, J. Li, J. Xu, M. Zhu and Y.-F. Han, *Green Energy Environ.*, 2023, **8**, 444-451.
9. S. Jia, Z. Dong, Z. Wang, B. Shen and H. Lyu, *J. Environ. Chem. Eng*, 2024, **12**, 114130.
10. X. Yang, J. Cheng, X. Xuan, N. Liu and J. Liu, *ACS Sustainable Chem. Eng.*, 2020, **8**, 10536-10543.
11. J. Li, F. Zhang, X. Zhan, H. Guo, H. Zhang, W.-Y. Zan, Z. Sun and X.-M. Zhang, *Chin. J. Catal.*, 2023, **48**, 117-126.
12. M. Liu, X. Zhao, S. Yang, X. Yang, X. Li, J. He, G. Z. Chen, Q. Xu and G. Zeng, *ACS Appl. Mater. Interfaces*, 2023, **15**, 44384-44393.
13. S. Gong, W. Wang, R. Lu, M. Zhu, H. Wang, Y. Zhang, J. Xie, C. Wu, J. Liu, M. Li, S. Shao, G. Zhu and X. Lv, *Appl. Catal., B*, 2022, **318**, 121813.